HHS Public Access

Author manuscript

Science. Author manuscript; available in PMC 2019 January 20.

Published in final edited form as:

Science. 2018 July 20; 361(6399): 290–295. doi:10.1126/science.aap8411.

VHL Substrate Transcription Factor ZHX2 As An Oncogenic Driver In Clear Cell Renal Cell Carcinoma

Jing Zhang[1,15,16], **Tao Wu**[2,16], **Jeremy Simon**[1,3], **Mamoru Takada**[1], **Ryoichi Saito**[1], **Cheng Fan**[1], **Xian-De Liu**[4], **Eric Jonasch**[4], **Ling Xie**[5], **Xian Chen**[5], **Xiaosai Yao**[6,7], **Bin Tean Teh**[7,8,9], **Patrick Tan**[6,9], **Xingnan Zheng**[1], **Mingjie Li**[1], **Cortney Lawrence**[1], **Jie Fan**[10], **Jiang Geng**[11], **Xijuan Liu**[1], **Lianxin Hu**[1], **Jun Wang**[1], **Chengheng Liao**[1], **Kai Hong**[1], **Giada Zurlo**[1], **Joel S. Parker**[1], **J. Todd Auman**[1], **Charles M. Perou**[1], **W. Kimryn Rathmell**[12], **William Y. Kim**[1], **Marc W. Kirschner**[2], **William G. Kaelin Jr**[13], **Albert S. Baldwin**[1], and **Qing Zhang**[1,14,15]

[1]Lineberger Comprehensive Cancer Center, University of North Carolina School of Medicine, Chapel Hill, NC 27599, USA

[2]Department of Systems Biology, Harvard Medical School, Boston, MA 02115, USA

[3]Department of Genetics, Neuroscience Center, University of North Carolina, Chapel Hill, NC 27599, USA

[4]Departments of Genitourinary Medical Oncology, The University of Texas MD Anderson Cancer Center, Houston, TX 77030, USA

[5]Department of Biochemistry and Biophysics, University of North Carolina, Chapel Hill, NC 27599, USA

[6]Cancer Therapeutics and Stratified Oncology, Genome Institute of Singapore, Singapore 138672, Singapore

[7]Institute of Molecular and Cell Biology, Singapore 138673, Singapore

[8]Laboratory of Cancer Epigenome, Department of Medical Sciences, National Cancer Centre, Singapore 169610, Singapore

[9]Cancer and Stem Cell Biology Program, Duke-NUS Medical School, Singapore 169857, Singapore

[10]Department of Pathology, Huashan Hospital, Fudan University, Shanghai, China

[11]Department of Urology, Shanghai Tenth People's Hospital, Tongji University, Shanghai, China

Corresponding author: Qing_Zhang@med.unc.edu.

Authors contributions: Q.Z., J.Z. and T.W. conceived the project. J.Z., T.W., M.T., R.S., X.L., L.X., X.Z., C.L., X.L., L.H., J.W., C.L., K.H., G.Z. and Q.Z. performed experiments. C.F. performed the patient data analysis. J.F. and J.G. performed TMA IHC staining quantification. J.P. and T.A. performed tumor sample sequencing and analysis. E.J., X.C., C.P., W.R., W.K., M.K., W.G.K. and A.B. helped supervising the study and providing critical advice and reagents for the paper. X.Y., B.T. and P.T. provided the unpublished histone ChIP-Seq data set. J.S. provided all of bioinformatics analysis. M.L. provided helps on obtaining patient samples in kidney cancer. J.Z., W.G.K., A.B. and Q.Z. wrote the manuscript with critical comments from all authors.

Competing interests: The authors declare no conflicts of interest.

Data and materials availability: Additional data are available in the supplementary materials. The ChIP-seq data and microarray data are available at the Gene Expression Omnibus under accession numbers GSE109953 and GSE110094.

[12]Division of Hematology and Oncology, Department of Medicine, Vanderbilt-Ingram Cancer Center, Vanderbilt University Medical Center, Nashville, Tennessee 37232, USA

[13]Howard Hughes Medical Institute, Department of Medical Oncology, Dana-Farber Cancer Institute, Harvard Medical School, Boston, MA 02215, USA

[14]Department of Pharmacology, University of North Carolina, Chapel Hill, NC 27599, USA

[15]Department of Pathology and Laboratory Medicine, University of North Carolina, Chapel Hill, NC 27599, USA

[16]These authors contributed equally

Abstract

Inactivation of the von Hippel-Lindau (*VHL*) E3 ubiquitin ligase protein is a hallmark of clear cell renal cell carcinoma (ccRCC). Identifying how pathways affected by VHL loss contribute to ccRCC remains challenging. We used a genome-wide *in vitro* expression strategy to identify proteins that bound VHL when hydroxylated. Zinc fingers and homeoboxes 2 (ZHX2) was found as a VHL target and its hydroxylation allowed VHL to regulate its protein stability. Tumor cells from ccRCC patients with *VHL* loss-of-function mutations usually had increased abundance and nuclear localization of ZHX2. Functionally, depletion of ZHX2 inhibited VHL-deficient ccRCC cell growth *in vitro* and *in vivo*. Mechanistically, integrated ChIP-Seq and microarray analysis showed that ZHX2 promoted NF-κB activation. These studies reveal ZHX2 as a potential therapeutic target for ccRCC.

One Sentence Summary

A genome-wide screen identified ZHX2 as a hydroxylation-dependent VHL substrate that promotes NF-κB activity and ccRCC tumorigenesis

---

ccRCC makes up approximately 70% of all renal malignancies and up to 92% of these cancers have inactivated the *VHL* gene (*1, 2*). Therapies that indirectly target the canonical VHL substrate HIF, such as vascular endothelial growth factor (VEGF) inhibitors, are the standard of care for ccRCC but drug resistance occurs in most patients (3). Therefore, identification of additional VHL substrates could improve therapeutic options for ccRCC.

Prolyl hydroxylation of HIFα paralogs by EglN family proteins promotes their binding with the VHL complex (VBC, including VHL and elongin B and C), which leads to their ubiquitination and degradation (*4–7*). Other potential VHL targets might undergo similar prolyl hydroxylation. Therefore, hydroxylated (p-OH), but not non-hydroxylated HIF1α peptide should compete with potential VHL targets for binding with VBC. We validated this by incubating ^{35}S-labeled HIF2α protein with Glutathione S-transferase VBC (GST-VBC) in the presence of p-OH HIF1α peptide in a competition assay (fig. S1A). Next, a genome-wide human cDNA library was divided into approximately 700 pools with 24 cDNAs/pool (8), which were *in vitro* translated followed by binding assays with the GST-VBC in the presence of either unmodified or p-OH HIF1α peptide. Pools containing a potential binding partner were further analyzed to identify individual proteins (Fig. 1A). We mixed the HIF2α cDNA with a cDNA pool and found that even in the ratio of 33:1 (cDNA pool: HIF2α),

HIF2α can be retrieved as a positive hit (fig. S1B). We discovered a pool that contained a protein whose binding to VBC was displaced by the p-OH HIF1α peptide and identified ZHX2 as the relevant protein in the pool (Fig. 1B-C). Similar to HIF2α, the prolyl hydroxylase inhibitors dimethyloxalylglycine (DMOG), deferoxamine (DFO), or $CoCl_2$ inhibited binding of ZHX2 to GST-VBC (Fig. 1D).

ZHX2 was reported to be a tumor suppressor in hepatocellular carcinoma (HCC) and lymphoma (*9, 10*). Recently, mRNA levels of its related family members ZHX1 and ZHX3 were reported to associate with the pathological stage of ccRCC (11). The amount of ZHX2 protein, but not ZHX1 or 3, in VHL-deficient ccRCC cells decreased if VHL was reintroduced (fig. S1C-D) and inhibition of prolyl hydroxylation or proteasomal degradation increased ZHX2 protein levels (**Fig. 1E-F,** fig. S1E). ZHX2 was predominantly localized in the nucleus (fig. S1F). Prolyl hydroxylation inhibition led to decreased binding of ZHX2 to VHL (**Fig. 1G,** fig. S1G). DMOG, DFO, proteasomal inhibitor MG132, and CRISPR/Cas9-mediated elimination of VHL increased the abundance of ZHX2 protein in VHL-proficient human kidney cells (fig. S1H-J). Conversely, reintroduction of VHL into VHL-deficient ccRCC cells increased the ubiquitination and degradation of endogenous ZHX2 (Fig.1H). Similar effects were observed with exogenous ZHX2 (Fig.1I, fig.S1K-M). Thus, ZHX2 is regulated by VHL through prolyl hydroxylation and proteasomal degradation. Next, we performed mass spectrometry and identified three ZHX2 prolyl hydroxylation sites: proline 427, 440, and 464 (fig. S2A-E). We generated single proline-to-alanine mutants (P427A, P440A, and P464A) and a triple mutant that harbors three mutations (P3A). The single mutants, and especially the P3A mutant, exhibited decreased VHL binding, ubiquitination and a concomitant increase of ZHX2 (Fig.1J-K, fig. S2F-G). The sensitivity of the single mutants to VHL was variable in different ccRCC cell lines (fig. S2F-G). The significance of this is unclear but may reflect cell line-dependent differences on hydroxylating the remaining prolyl hydroxylation sites due to variable expression of relevant hydroxylase(s).

We obtained 7 tumors from ccRCC patients and confirmed *VHL* loss of function mutations important for HIFα regulation in all 7 by sequencing (*2, 12–15*) (Table S1), most of which contained greater amounts of ZHX2, HIF1α and HIF2α than the paired normal tissues (Fig. 2A). For two tumors with *VHL* missense mutations (332 and 778), we did not observe distinctive upregulation of ZHX2 compared to normals, possibly because such mutations are less critical for ZHX2 regulation. Normal kidney tissues contained variable amount of ZHX2, HIF1α and HIF2α, which could be due to tissue heterogeneity or some degree of tumor contamination. In some cases, protein levels of ZHX2 and HIFα did not correlate with one another, possibily because of distinct VHL-independent regulatory pathways. ZHX2, HIF1α and HIF2α upregulation were also found for another two pairs of ccRCC tumor tissues harboring *VHL* frameshift mutations (Table S1), but not ccRCC tumors with intact VHL (Fig. 2B). Despite the lack of ZHX2 protein by western blot, ZHX2 displayed cytoplasmic and apical membrane immunohistochemical staining patterns in normals, similar to HIF2α. This discrepancy remains to be resolved. On the other hand, ZHX2 was exclusively in the nucleus of tumors harboring *VHL* frameshift mutations (fig. S3A-C, Fig. 2C). These findings were corroborated using ccRCC tissue microarray (**Fig. 2D-E,** Table

S2). Thus, VHL loss usually increases the abundance and nuclear levels of ZHX2 in ccRCC tumors.

Depletion of ZHX2 in multiple VHL-deficient ccRCC cells with several independent shRNAs or sgRNAs decreased cell proliferation and growth in soft agar (**Fig. 3A-F,** fig. S4A-G and fig. S5A-H). These phenotypic defects were rescued by exogenously expressing shRNA-resistant or sgRNA-resistant ZHX2 cDNAs respectively (**Fig. 3G-I,** fig. S4H-I **and** fig. S5I-M). These rescues were incomplete, however, possibly because the exogenous ZHX2 was incompletely localized to nuclei compared to endogenous ZHX2 (fig. S4J). In addition, ZHX2 depletion decreased orthotopic tumor growth (**Fig. 3J-K,** fig. S6A). To ask if ZHX2 was required for established tumors, we introduced two doxycycline-inducible ZHX2 shRNAs into 786-O cells. Depletion of ZHX2 in the presence of doxycycline correlated with decreased cell proliferation *in vitro* (fig. S6B-C). Next, 786-O cells expressing either ZHX2 shRNAs (45) cells or the control were injected into the renal capsules of immuno-deficient mice. Upon tumor formation, mice were fed doxycycline. Whereas cells expressing control shRNA grew readily after 6 weeks, cells expressing ZHX2 shRNA failed to proliferate, as determined by serial *in vivo* live tumor imaging and tumor-bearing kidney weights at necropsy (**Fig. 3L-M,** fig. S6D-E).

Next, we performed gene expression profiling of 786-O cells after ZHX2 knockdown followed by gene set enrichment analysis (GSEA) adjusted for gene function associated with oncogenic pathways. ZHX2 depletion caused decreased expression of multiple genes linked with anti-apoptosis, cell proliferation, invasion/metastasis, and metabolism (fig. S7A-F). Interestingly, GSEA analyses also demonstrated that NF-κB activity was suppressed by ZHX2 depletion (fig. S8A-B). Real time PCR (RT-PCR) analysis confirmed that ZHX2 depletion decreased the expression of canonical NF-κB target genes, including c-c motif chemokine ligand 2 (*CCL2*), interleukin-8 (*IL8)* and interleukin 6 (*IL6)* (Fig. 4A). Generally, the more effective ZHX2 shRNA (sh45) suppressed the NF-κB-responsive mRNAs better. The *CCL2* and *IL8* mRNAs were, however, profoundly suppressed by both ZHX2 shRNAs, possibly because both shRNAs suppressed NF-κB below a threshold required for these two mRNAs (Fig. 4A).

Loss of *VHL* constitutively activates the NF-κB pathway (*16–18*). NF-κB activation is characterized by degradation of IκBα and phosphorylation of RelA/p65, which then accumulates in the nucleus (*19–21*). Depletion of ZHX2 had no significant effect on IκB degradation or RelA/p65 phosphorylation but inhibited translocation of RelA/p65 into the nucleus (**Fig. 4B,** fig. S8C-D). We detected binding of ZHX2 to RelA/p65 with endogenous and exogenous proteins (**Fig. 4C,** fig. S8E-F). In contrast, we have thus far not detected binding of ZHX2 to other NF-κB subunits (fig. S8F). Inhibiting NF-κB with RelA/p65 shRNAs or with a specific IKK inhibitor compound A (CMPDA) suppressed VHL-deficient ccRCC cell proliferation and growth in soft agar (fig. S9A-L) (22). We performed chromatin immunoprecipitation followed by high-throughput sequencing (ChIP-seq) to determine genome-wide chromatin occupancy of ZHX2 and RelA/p65, which revealed that 75% of p65 binding sites overlapped with those of ZHX2 (**Fig. 4D and** fig. S10A-B). ChIP-qPCR confirmed the binding by ZHX2 and p65 at the promoters of several genes (fig. S10C-D). DNA sequences bound by both NF-κB-p65 and ZHX2 were enriched for the NF-κB

consensus motif (fig. S10E). ZHX2 and RelA/p65 overlapping sites also displayed a strong enrichment for H3K4me3 and H3K27ac, but not H3K4me1 (Fig. 4E) (23), indicating that ZHX2 and RelA/p65 bound to active gene promoters. Interestingly, ZHX2 and HIF2α positively regulated genes showed minimal overlap (fig. S11A. Table S3), and Gene Ontology (GO) analysis showed that ZHX2 regulated distinct pathways including NF-κB (fig. S11B). Integrated analyses of ZHX2 and NF-κB-p65 localization and gene expression showed 390 genes regulated by both ZHX2 and RelA/p65 positively (**Fig. 4F,** Table S4), among which higher expression of 32 genes was associated with a worse prognosis for ccRCC patients (Fig. 4G, and Table S5). These 32 genes were further analyzed by hierarchical clustering analysis of The Cancer Genome Atalas (TCGA) RCC cases which showed that 18 had high correlations with each other (Fig. S12A). A metagene representing the median expression of these 18 was a very strong predictor of a worse prognosis (fig. S12B). ZHX2 depletion impaired RelA/p65 occupancy on *IL6* and inhibitor of NF-κB kinase subunit epsilon (*IKBKE)* promoters (Fig. 4H). VHL binding-defective ZHX2 promoted ccRCC cell growth on soft agar, with this effect ameliorated by CMPDA treatment (fig. S13A-B). Thus, our results suggest that ZHX2 promotes NF-κB activation and ccRCC carcinogenesis.

HIF2α and its downstream targets [such as VEGF, glucose transporter member 1 (GLUT1), perilipin (PLIN2) and c-Myc] contribute to ccRCC (*3, 24–26*). However, the HIF2α inhibitor PT2399 is effective in only a subset of ccRCC (*27, 28*). We found ZHX2 depletion or IKK inhibition inhibited soft agar growth of UMRC2 and UMRC6 cells (Fig.3, fig. S4, S5 **and** S9) whereas inhibition or depletion of HIF2α did not (27). ZHX2 has been reported to be an HCC tumor suppressor and to repress Cyclin A, Cyclin E, alpha fetoprotein (AFP) and multidrug resistance 1 (MDR1) expression (*10, 29, 30*). We did not detect suppression of these mRNAs in ccRCC cells (fig. S14). ZHX2 targets may be context dependent, thereby allowing it to act as an oncoprotein in ccRCC. The oncogenic role of ZHX2, via control of NF-κB activation, might provide additional therapeutic avenues for ccRCC.

Supplementary Material

Refer to Web version on PubMed Central for supplementary material.

Acknowledgments

The initial screen was performed in Kaelin lab when Q.Z was a postdoctoral fellow. We thank all members of the Zhang, Kaelin and Baldwin labs for helpful discussions and suggestions, G.Wang for help with ChIP-Seq, W.Yu for providing VHL sgRNAs, UNC Tissue Procurement Facility, and UNC Translational Pathology Laboratory.

Funding: This work was supported in part by Department of Defense (DoD) Career Development Award (Q.Z., W81XWH-15–1-0599), University Cancer Research Fund innovator award (J.Z), NINDS-P30NS045892 (J.S), National Cancer Institute (Q.Z., R01CA211732, R21CA223675) and (A.B., R35CA197684). Q.Z is a V Scholar, Kimmel Scholar, Susan G. Komen Career Catalyst awardee and Mary Kay Foundation awardee. J.Z. is supported by a DoD Fellowship Award (W81XWH-17–1-0016). WGK is an HHMI investigator and is supported by R35 CA210068 from NCI. XY is supported by National Medical Research Council (OFYIRG17May057) and Biomedical Research Council (BRMC YIG Grant No: 1510851024) from Singapore.

References and Notes

1. Hsieh JJ et al., Nat Rev Dis Primers 3, 17009 (2017). [PubMed: 28276433]

2. Sato Y et al., Nat Genet 45, 860–867 (2013). [PubMed: 23797736]
3. Escudier B, Szczylik C, Porta C, Gore M, Nat Rev Clin Oncol 9, 327–337 (2012). [PubMed: 22473096]
4. Min JH et al., Science 296, 1886–1889 (2002). [PubMed: 12004076]
5. Epstein AC et al., Cell 107, 43–54 (2001). [PubMed: 11595184]
6. Jaakkola P et al., Science 292, 468–472 (2001). [PubMed: 11292861]
7. Ivan M et al., Science 292, 464–468 (2001). [PubMed: 11292862]
8. Ayad NG, Rankin S, Ooi D, Rape M, Kirschner MW, Methods Enzymol 399, 404–414 (2005). [PubMed: 16338372]
9. Nagel S et al., Leuk Res 36, 646–655 (2012). [PubMed: 22078940]
10. Yue X et al., Gastroenterology 142, 1559–1570 e1552 (2012). [PubMed: 22406477]
11. Kwon RJ et al., PLoS One 12, e0171036 (2017). [PubMed: 28152006]
12. Ma X, Yang K, Lindblad P, Egevad L, Hemminki K, Oncogene 20, 5393–5400 (2001). [PubMed: 11536052]
13. Razafinjatovo C et al., BMC Cancer 16, 638 (2016). [PubMed: 27530247]
14. Miller F, Kentsis A, Osman R, Pan ZQ, J Biol Chem 280, 7985–7996 (2005). [PubMed: 15611064]
15. Stebbins CE, Kaelin WG, Jr., Pavletich NP, Science 284, 455–461 (1999). [PubMed: 10205047]
16. An J, Rettig MB, Molecular and cellular biology 25, 7546–7556 (2005). [PubMed: 16107702]
17. Qi H, Ohh M, Cancer Res 63, 7076–7080 (2003). [PubMed: 14612498]
18. Yang H et al., Mol Cell 28, 15–27 (2007). [PubMed: 17936701]
19. Ghosh S, Hayden MS, Immunol Rev 246, 5–13 (2012). [PubMed: 22435544]
20. Perkins ND, Nat Rev Cancer 12, 121–132 (2012). [PubMed: 22257950]
21. Staudt LM, Cold Spring Harb Perspect Biol 2, a000109 (2010). [PubMed: 20516126]
22. Hutti JE et al., Cancer Res 72, 3260–3269 (2012). [PubMed: 22552288]
23. Yao X et al., Cancer Discov 7, 1284–1305 (2017). [PubMed: 28893800]
24. Gordan JD et al., Cancer Cell 14, 435–446 (2008). [PubMed: 19061835]
25. Qiu B et al., Cancer Discov 5, 652–667 (2015). [PubMed: 25829424]
26. Chan DA et al., Sci Transl Med 3, 94ra70 (2011).
27. Cho H et al., Nature 539, 107–111 (2016). [PubMed: 27595393]
28. Chen W et al., Nature 539, 112–117 (2016). [PubMed: 27595394]
29. Ma H et al., Oncotarget 6, 1049–1063 (2015). [PubMed: 25473899]
30. Shen H et al., J Cell Mol Med 12, 2772–2780 (2008). [PubMed: 18194454]
31. Li L et al., Mol Cell Biol 27, 5381–5392 (2007). [PubMed: 17526729]
32. Yang H, Ivan M, Min JH, Kim WY, Kaelin WG, Jr., Methods in enzymology 381, 320–335 (2004). [PubMed: 15063684]
33. Wang D, Baldwin AS, Jr., The Journal of biological chemistry 273, 29411–29416 (1998). [PubMed: 9792644]
34. Kendellen MF, Bradford JW, Lawrence CL, Clark KS, Baldwin AS, Oncogene 33, 1297–1305 (2014). [PubMed: 23474754]
35. Zhang Q et al., Cancer Cell 16, 413–424 (2009). [PubMed: 19878873]
36. Zhang J, Hu MM, Wang YY, Shu HB, J Biol Chem 287, 28646–28655 (2012). [PubMed: 22745133]
37. Chen X et al., Nature 508, 103–107 (2014). [PubMed: 24670641]
38. Lu R et al., Cancer cell 30, 92–107 (2016). [PubMed: 27344947]
39. Zhang Y et al., Genome biology 9, R137 (2008). [PubMed: 18798982]
40. Lassmann T, Hayashizaki Y, Daub CO, Bioinformatics 25, 2839–2840 (2009). [PubMed: 19737799]
41. Wu TD, Nacu S, Bioinformatics 26, 873–881 (2010). [PubMed: 20147302]
42. Encode Project Consortium Nature 489, 57–74 (2012). [PubMed: 22955616]
43. Heinz S et al., Molecular cell 38, 576–589 (2010). [PubMed: 20513432]

44. Therneau TM, Grambsch PM, Statistics for biology and health (Springer, New York, 2000), pp. xiii, 350 p.
45. Harrell FE, Jr., Lee KL, Califf RM, Pryor DB, Rosati RA, Stat Med 3, 143–152 (1984). [PubMed: 6463451]
46. Li L et al., Cancer Cell 24, 738–750 (2013). [PubMed: 24332042]
47. Zhang J et al., EMBO J 34, 2953–2970 (2015). [PubMed: 26492917]
48. Zhao X et al., PloS one 10, e0129280 (2015). [PubMed: 26076459]
49. Liu XD et al., Oncogene 34, 2450–2460 (2015). [PubMed: 24998849]
50. Han CP et al., Mod Pathol 22, 797–806 (2009). [PubMed: 19347018]
51. Seifert BA et al., Clin Cancer Res 22, 4087–4094 (2016). [PubMed: 27083775]
52. Huang da W, Sherman BT, Lempicki RA, Nat Protoc 4, 44–57 (2009). [PubMed: 19131956]

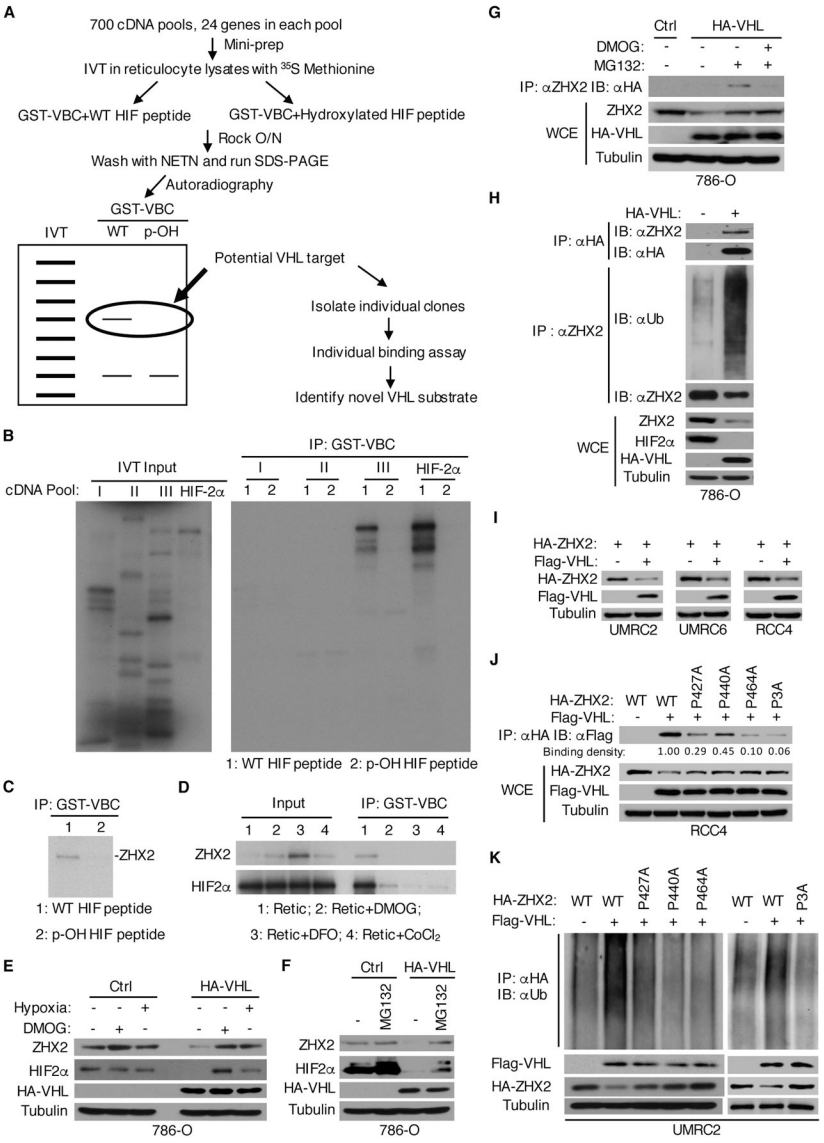

Figure 1. ZHX2 is a VHL target and its stability is regulated through prolyl hydroxylation

(A) Schematic representation of VHL substrate screen.

(B-C) Binding assays of ^{35}S-Methionine labelled in vitro translated cDNA pools (B) or ZHX2 (C) and GST-VBC in the presence of wildtype (WT) or prolyl hydroxylated (p-OH) HIF peptide.

(D) ZHX2/HIF2α binding to GST-VBC in the presence of prolyl hydroxylase inhibitors.

(E-H) Immunoblots (IB) of whole cell extracts (WCE) and immunoprecipitations (IP) of lysates from 786-O cells infected with lentivirus encoding either control vector (Ctrl) or hemagglutinin (HA) tagged VHL and treated as indicated for 8 h.

(I) IB of lysates from UMRC2, UMRC6, or RCC4 cells transfected with indicated plasmids.

(J-K) IB of WCE and IP of RCC4 cells transfected with indicated plasmids followed by densitometry analysis of Flag-VHL (J) or ubiquitination assays in UMRC2 cells transfected with indicated plasmids (K).

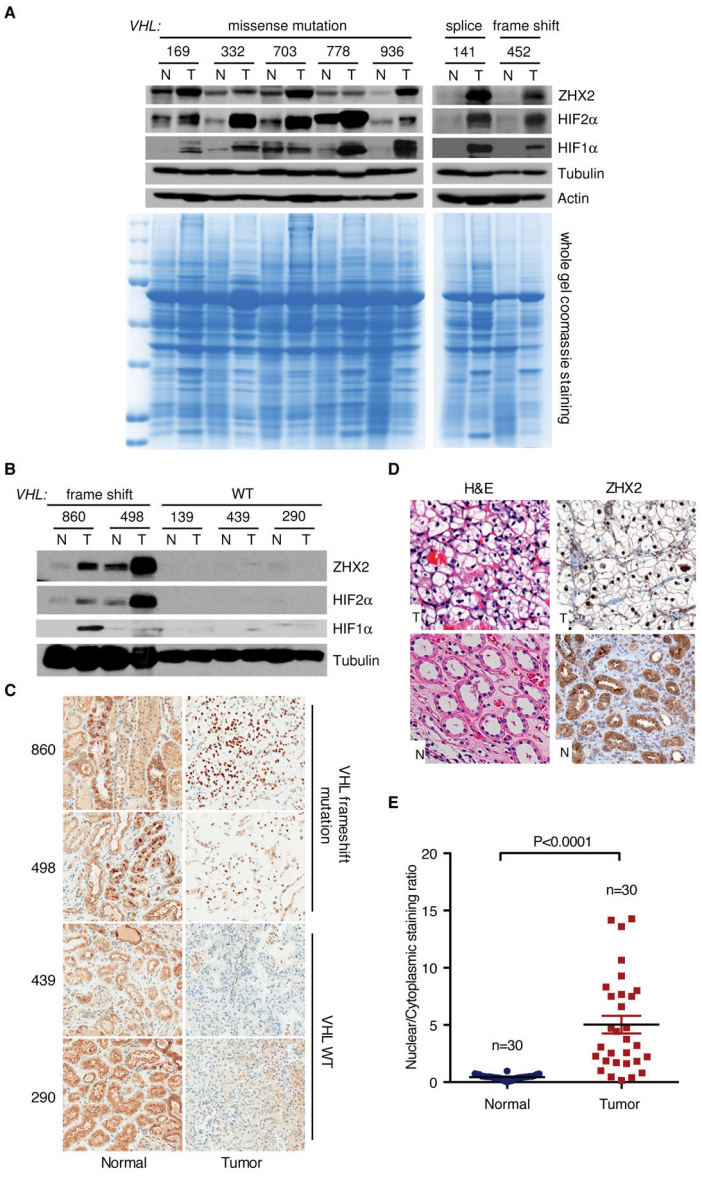

Figure 2. ZHX2 accumulation in ccRCC patients

(A–B) IB of lysates from paired ccRCC patient non-tumor (N) and tumor (T) tissues.

(C) Representative ZHX2 immunohistochemistry staining for ccRCC patient tissues.

(D-E) Representative H&E, ZHX2 immunohistochemistry staining of tumor (T) and non-tumor (N) tissues (D) and quantification of ZHX2 nuclear/cytoplasmic staining ratio (E) from ccRCC TMA slides. Error bars represent SEM (unpaired *t*-test).

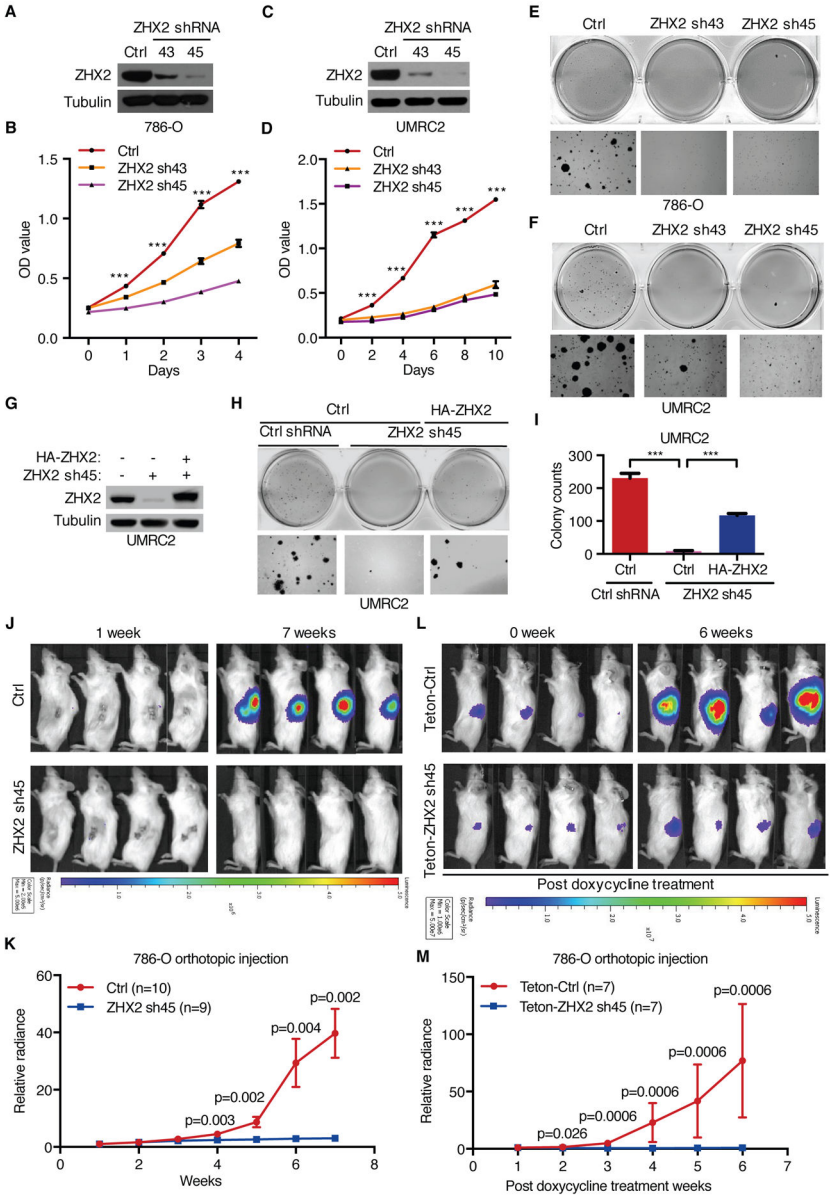

Figure 3. Requirement of ZHX2 for ccRCC cell proliferation, anchorage-independent growth and tumorigenesis

(A-F) IB of cell lysates (A, C), cell proliferation (B, D) and soft agar growth (E, F) of 786-O and UMRC2 cells infected with lentivirus encoding control (Ctrl) or ZHX2 shRNAs (43, 45) (N=3). See fig. S4A-B for soft agar quantitation results.

(G-I) IB of cell lysates (G) and representative soft agar growth assays (H) and their quantification (I) of UMRC2 cells transfected with ZHX2 sh45-resistant HA-ZHX2 or control (Ctrl) vector, followed by ZHX2 sh45 or control (Ctrl) shRNA infection (N=3).

(J-M) Representative bioluminescence imagings of 1 and 7 weeks post-implantation (J) and quantification of bioluminescence imaging (K) from 786-O cells luciferase stable cells infected with either ZHX2 sh45 or control (Ctrl) shRNA, or imagings of 0 week and 6 weeks post-doxycycline treatment (L) and quantification of imaging (M) from 786-O

luciferase stable cells infected with lentivirus encoding either Teton-ZHX2 sh45 or Teton-control (Teton-Ctrl) shRNA injected orthotopically into the renal sub-capsule of NOD scid gamma (NSG) mice as indicated. The Mann-Whitney test was used to calculate the p values. Error bars represent SEM, ***$P<0.001$ (unpaired t-test) in panel B, D and I.

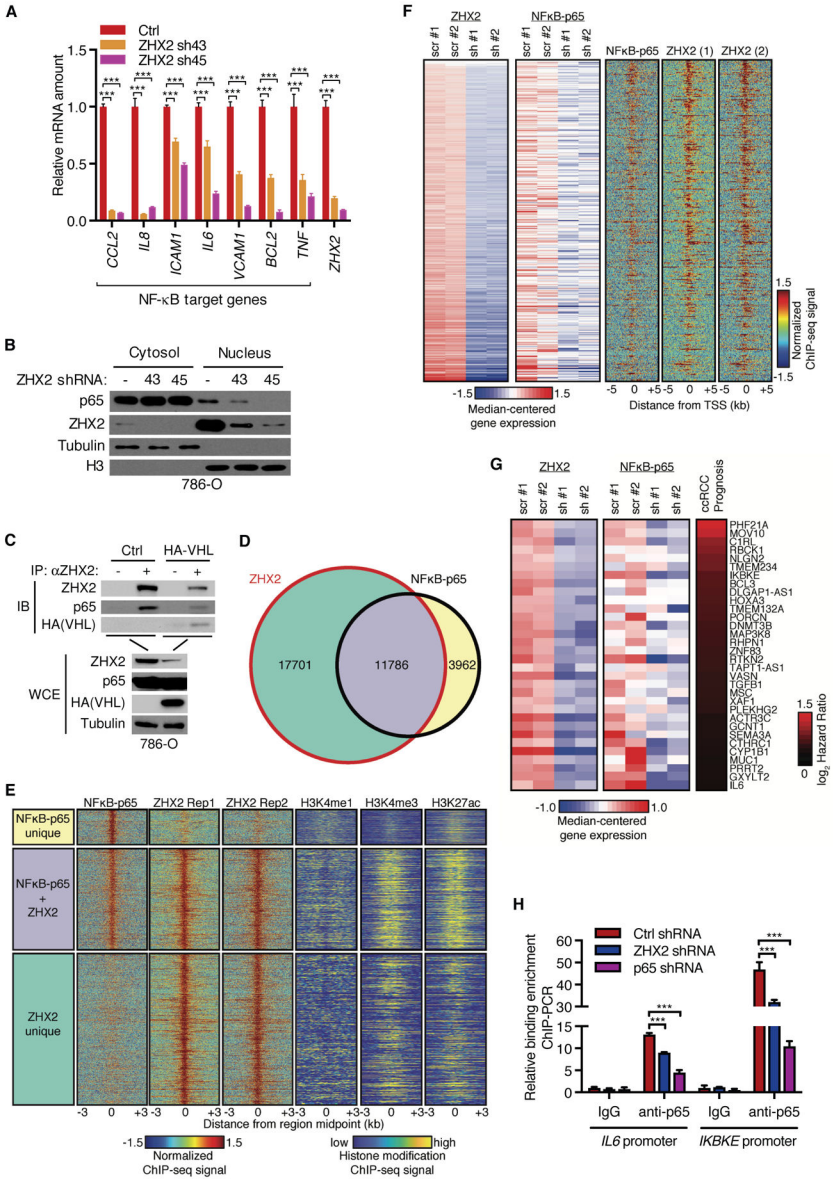

Figure 4. ZHX2 regulates NF-κB activation

(A-B) qRT-PCR quantification of mRNA of NF-κB target genes (A, N=3) or IB of cell fractions (B) from 786-O cells infected with ZHX2 shRNAs (43, 45) or Ctrl.

(C) IB of WCE and IP of 786-O cells infected with either Ctrl or HA-VHL.

(D) Venn diagram showing ChIP-Seq binding peak overlap between ZHX2 and NF-κB–p65. ZHX2 ChIP-seq experiments were performed in duplicate and intersected.

(E) ChIP-seq signal intensity in the 3 kb surrounding the midpoint of unique ZHX2 (green), unique NF-κB–p65 (yellow), and common (purple) sites.

(F) Heatmap for genes downregulated due to ZHX2 and p65 silencing (adj. $P < 0.05$) are shown.

(G) Heatmap for activated genes that were strongly bound by both ZHX2 and NF-κB–p65 and were significantly associated with ccRCC prognosis ($q < 0.01$). The log2 Cox Hazard Ratio was colored red (higher expression associated with poorer prognosis).

(H) ChIP-qPCR of NF-κB–p65 binding at *IL6* and *IKBKE* promoters following silencing of indicated genes (N=3).

Error bars represent SEM, ***$P<0.001$ (unpaired t-test).